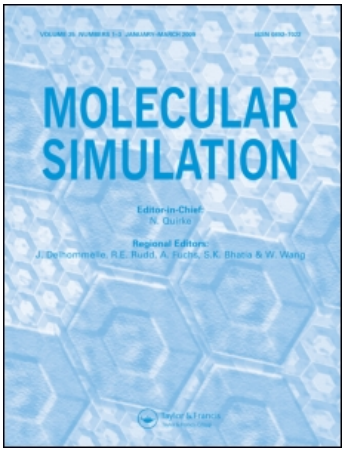

Molecular Simulation
Publication details, including instructions for authors and subscription information:
http://www.informaworld.com/smpp/title~content=t713644482

An Effective Potential for Adsorption of Polar Molecules on Graphite

Xiongce Zhao[a]; J. Karl Johnson[ab]
[a] Department of Chemical and Petroleum Engineering, University of Pittsburgh, Pittsburgh, PA, USA [b] US Department of Energy, National Energy Technology Laboratory, Pittsburgh, PA, USA

To cite this Article Zhao, Xiongce and Johnson, J. Karl(2005) 'An Effective Potential for Adsorption of Polar Molecules on Graphite', Molecular Simulation, 31: 1, 1 — 10
To link to this Article: DOI: 10.1080/0892702042000272889
URL: http://dx.doi.org/10.1080/0892702042000272889

Molecular Simulation, VOL. 31 (1), 15 January 2005, pp. 1–10

An Effective Potential for Adsorption of Polar Molecules on Graphite

XIONGCE ZHAO[a] and J. KARL JOHNSON[a,b,*]

[a]*Department of Chemical and Petroleum Engineering, University of Pittsburgh, Pittsburgh, PA 15261, USA;* [b]*National Energy Technology Laboratory, US Department of Energy, P.O. Box 10940, Pittsburgh, PA 15236, USA*

(Received July 2004; In final form July 2004)

Each carbon atom in the graphite crystal has a quadrupole moment due to the symmetry of the crystal. We show that these graphite quadrupoles, along with the polarizability of graphite, have a substantial effect on adsorption of strongly polar molecules. We present an approximate method for accounting for the change in the solid–fluid potential energy due to polar interactions with graphite. The potential function is integrated over the graphite surface using a truncated Fourier series, so that the resulting potential is analogous to the Steele 10-4-3 potential. The interactions included in this potential include dipole-induced dipole, dipole–quadrupole, and quadrupole–quadrupole interactions. Hence, the potential can be used for fluid molecules with dipole and/or quadrupole moments. Fluid–fluid multipole interactions can be computed with any model; but point multipoles must be used in the solid–fluid potential. The multipole solid–fluid potential is most accurate for nearly spherical molecules.

Keywords: Adsorption; Polar molecules; Graphite; Graphite quadrupole moment

INTRODUCTION

Molecular simulation of gas adsorption on graphitic sorbents requires accurate and computationally efficient descriptions of the solid–fluid potential energy surfaces (PES). For years people have been using the analytically smoothed (integrated) potential developed by Steele [1] to model adsorption of fluids on graphite [2]. This so-called 10-4-3 potential accounts for the van der Waals dispersion and repulsion interaction between an adsorbate molecule and atoms in the graphite sorbent based on the Lennard–Jones (LJ) potential. It is known that each carbon atom in graphite has an effective quadrupole moment [3–7]. Nevertheless, it has been common practice to assume that the electrostatic interactions between adsorbed molecules and the graphite surface are negligible compared with the dispersion–repulsion energies [8]. We show in this paper that neglect of polar terms is not justified for strongly polar adsorbates.

Nicholson *et al.* examined the effect of the graphite quadrupole on the adsorption of rare gas atoms [3,4]. Vernov and Steele [5] estimated the quadrupole moment of each C atom in graphite from values of the quadrupole moments of benzene, naphalene, and anthracene. They developed expressions for charges, dipoles, and quadrupoles interacting with the point quadrupoles in a graphite surface. These expressions are angle and position dependent. They found that in the case of H_2O on graphite the inclusion of the graphite quadrupoles significantly changed the PES. Whitehouse and Buckingham later experimentally measured the quadrupole moment of graphite and obtained a value of -3.03×10^{-40} C m^2 per carbon atom [6], which is about 30% smaller in magnitude than the value estimated by Vernov and Steele. Hansen and coworkers showed that N_2-graphite quadrupole terms are important to include in order to resolve discrepancies between experiments and model calculations for the dynamic properties of the N_2 monolayer on graphite [7]. We note that Hansen *et al.* constructed a value for the quadrupole moment per carbon based on X-ray diffraction intensities for bulk graphite from Chen *et al.* [9]. The value they obtained is 3.3×10^{-40} C m^2 [7], which is the same

*Corresponding author. E-mail: karlj@pitt.edu

ISSN 0892-7022 print/ISSN 1029-0435 online © 2005 Taylor & Francis Ltd
DOI: 10.1080/0892702042000272889

magnitude as the value measured by Whitehouse and Buckingham, but opposite in sign. In this work we used the value from Whitehouse and Buckingham [6] for all the computations.

In contrast to the work on the effect of the graphite quadrupole moment, there does not appear to be any work on the inclusion of the induction terms between a polar molecule and graphite. In this paper, we estimate the induction contribution to the adsorption potential and find that the dipole-induced dipole term can be as large as the dipole–quadrupole term. Thus, the polarizability of graphite is potentially as important as the quadrupole moment for the adsorption of polar molecules.

There are two general approaches to calculating the induction and multipole interactions between a polar adsorbate and graphite. We can use an atom-explicit potential to describe the interaction between an adsorbate molecule and each carbon atom in the graphite model, calculating the total energy by summing up all pairs of atoms. Dispersion, repulsion, electrostatic (multipole), and induction terms can all be computed in this way. But such an approach is computationally prohibitive for large systems. An alternate approach is to use an integrated potential that accounts for all the adsorbent atoms in an effective way. This has been a very popular and useful approach for modeling solid–fluid interactions for many systems, including graphite [10–13]. Integrated potentials, such as the 10-4-3 model for graphite, are computationally very efficient. There are no integrated potentials that account for multipole and induction energies for graphite.

In this paper, we present a set of integrated expressions that approximately account for graphite quadrupole interactions with adsorbate dipoles and quadrupoles. We also give expressions for the dipole-induced dipole term, where the induced dipole is located on the graphite carbon atoms. We compare the interaction energies from these expressions with those from atom-explicit potentials for a number of different polar fluids. We also compute adsorption isotherms and isosteric heats from potentials with and without the polar interactions and compare the calculated values. We demonstrate that the polar terms are very important for strongly polar fluids, while for weakly polar molecules the polar interactions may be neglected without loss of accuracy.

POTENTIAL DEVELOPMENT

We use the Fourier transformation approach developed by Steele [1] for non-polar interactions to derive integrated expressions for the multipole and induction interactions of polar adsorbate molecules interacting with graphite. The potential energy of a single fluid molecule interacting with a semi-infinite solid surface made up of periodically arranged atoms can be expressed as a Fourier series,

$$U(\mathbf{r}) = \sum_{\mathbf{g}} \sum_{n} w_g(z_n) \exp(i\mathbf{g}\cdot\boldsymbol{\tau}). \tag{1}$$

In Eq. (1), $\mathbf{r} = (x, y, z)$ denotes the position of an adsorbate molecule relative to the origin, where the origin is located at an arbitrary point in the solid surface. $\boldsymbol{\tau}$ is the two dimensional translation vector for x and y directions spanning the graphite surface. $\mathbf{g}$ is one of the set of the reciprocal lattice vectors defined to conform to the periodicity property of $U(r)$. $z_n = z + n\Delta$ is the distance along the solid surface normal direction from the adsorbate to a carbon atom in the n-th graphite sheet from the surface graphene layer. Δ is the distance between the graphene layers (see Fig. 1). An analytical expression for the Fourier coefficients $w_{\mathbf{g}}$ can be obtained from

$$w_{\mathbf{g}}(z_n) = \frac{1}{a_s}\int_{\mathbf{a}} \exp(-i\mathbf{g}\cdot\boldsymbol{\tau})\, u(z_n, \boldsymbol{\tau}) \mathrm{d}\boldsymbol{\tau}, \tag{2}$$

where $u(z_n,\boldsymbol{\tau})$ is the pairwise additive interaction potential between an adsorbate molecule and a carbon atom in graphite. a_s is the area of the graphene unit, and $\mathbf{a}$ denotes integration over the surface of graphite.

In the case where $u(z_n, \boldsymbol{\tau})$ is a function only of the separation distance between the fluid molecule and a solid atom, $r = (z_n^2 + x^2 + y^2)^{\frac{1}{2}}$ (see Fig. 1), we can integrate over the orientation of $\boldsymbol{\tau}$ to obtain

$$w_{\mathbf{g}}(z_n) = \frac{2\pi n_0}{a_s}\int_0^{\infty} J_0(\mathbf{g}t)\, u(r)\, t \mathrm{d}t, \tag{3}$$

where $t^2 = x^2 + y^2$, n_0 is the number of carbon atoms in a graphene unit cell, and J_0 is the Bessel function of

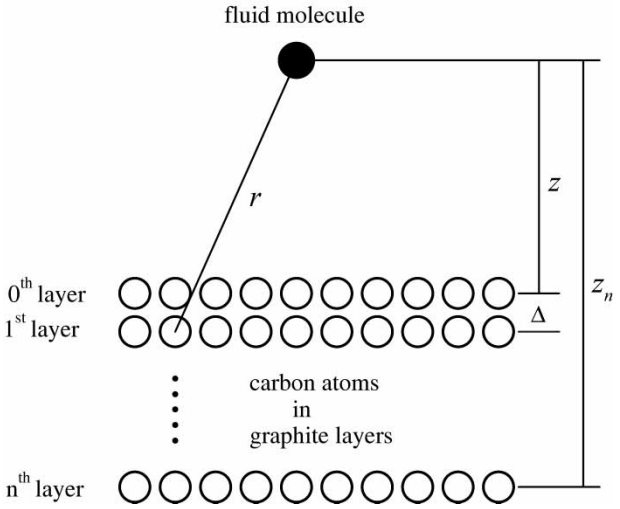

FIGURE 1 Schematic illustration of a fluid molecule interacting with the carbon atoms in graphite. The filled circle represents the fluid molecule and the open circles represent the carbon atoms in the graphene sheets.

the first kind. If $u(r)$ has an inverse power dependence on r, as is the case for the LJ potential, Eq. (3) can be integrated analytically. Substituting the integrated $w_{\mathbf{g}}$ back to Eq. (1) and summing over $\mathbf{g}$ we obtain a potential that is only a function of z_n. Details of the above derivation can be found in Ref. [10].

Steele [1] found that truncation of Eq. (1) to the $\mathbf{g} = \mathbf{0}$ term is sufficiently accurate to give excellent agreement with the explicit sum over the LJ sites when the corrugation of the potential does not need to be taken into account. He derived the well-known 10-4-3 potential by simplifying the truncated series further to obtain

$$U_{\mathrm{sf}}(z) = 2\pi\varepsilon_{\mathrm{sf}}\sigma_{\mathrm{sf}}^2\Delta\rho_{\mathrm{s}} \times \left[\frac{2}{5}\left(\frac{\sigma_{\mathrm{sf}}}{z}\right)^{10} - \left(\frac{\sigma_{\mathrm{sf}}}{z}\right)^{4} - \frac{\sigma_{\mathrm{sf}}^4}{3\Delta(0.61\Delta + z)^3}\right], \quad (4)$$

where z is the surface normal direction distance between a fluid molecule and the solid surface ($n = 0$ layer of graphite), $\rho_{\mathrm{s}} = n_0/(a_{\mathrm{s}}\Delta)$, and $\varepsilon_{\mathrm{sf}}$ and σ_{sf} are the cross interaction LJ potential parameters between the fluid and graphite. In Eq. (4), the z^{-10} and z^{-4} terms are derived from the $n = 0$ term in Eq. (1). Repulsive terms arising from the $n > 0$ layers are neglected. The last term in Eq. (4) is from the integration of the attractive term in the remainder of the layers. The value 0.61Δ rather than Δ is used in the last term because the integration of the $n > 0$ attractive terms from $z + 0.61\Delta$ was found to give a more accurate representation of the atom-explicit sum [1].

Similar procedures can be applied to obtain integrated expressions for induction and multipole interactions between a fluid molecule and graphite, as long as the pairwise potential satisfies two conditions: (1) The potential is a function only of the separation distance r. (2) The potential is short-ranged, i.e. the potential decreases as r^{-n} where $n > 1$. Both conditions are satisfied for angle averaged induction and multipole interaction potentials. This requires the use of point dipoles and point quadrupoles for the fluid–solid interactions.

Most potential models for polar molecules employ point charges to represent multipole moments rather than point multipole moments. The point charge representation may still be used to compute fluid–fluid interactions in a simulation, but the solid–fluid multipole potential must be approximated by point dipoles and quadrupoles within this formalism. The point multipole descriptions are needed in order to obtain an angle averaged potential that is only a function of the molecule separation. Using different multipole descriptions of the the fluid–fluid and solid–fluid interactions gives rise to an inconsistency in the overall description of the potential of the system. However, inclusion of the polar interactions at this level is a first order improvement over the general practice of ignoring the solid–fluid multipole interactions altogether.

We now present the atom-explicit formulas for the potentials of dipoles and quadrupoles in the fluid phase interacting with graphite. We will then develop integrated forms of these potentials that can be used directly in molecular simulations to approximate the fluid–graphite polar interactions without adding substantially to the computational cost of the simulation. The angle averaged dipole-induced dipole interaction potential is given by [14]

$$u_{\mu i}(r) = -\frac{\mu_{\mathrm{f}}^2\alpha_{\mathrm{c}}}{(4\pi\varepsilon_0)^2 r^6}, \quad (5)$$

where μ_{f} is the dipole moment of the fluid molecule, α_{c} is the angle averaged polarizability of a carbon atom in graphite, and ε_0 is the vacuum permittivity. Equation (5) does not account for self-consistency of the induced dipoles. This issue will be addressed in "Self-consistency" section. The angle averaged dipole–quadrupole interaction potential is [14]

$$u_{\mu\Theta}(r) = -\frac{\mu_{\mathrm{f}}^2\,\Theta_{\mathrm{c}}^2}{kT(4\pi\varepsilon_0)^2 r^8}, \quad (6)$$

where Θ_{c} is the quadrupole moment on each carbon atom in graphite, k is the Boltzmann constant and T is the absolute temperature.

Finally, we consider fluid molecules with quadrupoles interacting with graphite. We ignore the quadrupole-induced dipole term because it is much smaller than the quadrupole–quadrupole term. The angle averaged quadrupole–quadrupole potential is [14]

$$u_{\Theta\Theta}(r) = -\frac{14\Theta_{\mathrm{f}}^2\,\Theta_{\mathrm{c}}^2}{5kT(4\pi\varepsilon_0)^2 r^{10}}, \quad (7)$$

where Θ_{f} is the quadrupole moment of the fluid molecule.

Equations (6) and (7) were derived from their angle explicit counterparts using Boltzmann orientational averaging [14]. The accuracy of these expressions depends on the temperature. We will discuss the accuracy of Eqs. (5)–(7) in "Discussion on the angle average approach" section.

Substituting Eqs. (5)–(7) into Eq. (3) and integrating, we obtain the following expressions after simplifying the $\mathbf{g} = \mathbf{0}$ truncated series

$$U_{\mu i}(z) = -\frac{\Delta\rho_{\mathrm{s}}\pi\mu_{\mathrm{f}}^2\alpha_{\mathrm{c}}}{2(4\pi\varepsilon_0)^2}\left[\frac{1}{z^4} + \frac{1}{3\Delta(z+\Delta)^3}\right]. \quad (8)$$

Application of Eq. (8) to simulations involving many fluid molecules requires an additional assumption that the induction terms are pair-wise additive. Relaxing this assumption would preclude the use of an integrated potential. The integrated

dipole–quadrupole interaction potential is

$$U_{\mu\Theta}(z) = -\frac{\Delta\rho_s \pi \mu_f^2 \Theta_c^2}{3kT(4\pi\varepsilon_0)^2}\left[\frac{1}{z^6} + \frac{1}{5\Delta(z+\Delta)^5}\right]. \quad (9)$$

The integrated quadrupole–quadrupole interaction potential is

$$U_{\Theta\Theta}(z) = -\frac{7\Delta\rho_s \pi \Theta_f^2 \Theta_c^2}{10kT(4\pi\varepsilon_0)^2}\left[\frac{1}{z^8} + \frac{1}{7\Delta(z+\Delta)^7}\right]. \quad (10)$$

The potentials in Eqs. (8)–(10) are analogous to Steele's 10-4-3 potential in that they are only dependent on the z-direction distance between fluid molecules and the graphite surface. We have ignored the surface corrugation terms in the adsorbate–graphite interaction in order to obtain a simple expression that depends only on the distance from the graphite surface to the adsorbate. In contrast to the 10-4-3 function, we have not used an empirical adjustable parameter, such as 0.61 in Eq. (4), because the expressions are sufficiently accurate without the addition of an adjustable parameter.

DISCUSSION

Discussion on the Angle Average Approach

We have used angle averaged expressions for the induction and multipole interaction in the derivation of Eqs. (8)–(10). Equations (6) and (7) were obtained by using

$$\overline{u}_{ab} = \frac{\int\int u_{ab} \exp(-u_{ab}/kT)\, d\omega_a d\omega_b}{\int\int \exp(-u_{ab}/kT)\, d\omega_a d\omega_b} \quad (11)$$

to average the interaction energy between molecules a and b with relative distance r_{ab} held fixed [14]. The Boltzmann weighting factor $\exp(-u_{ab}/kT)$ is included to account for the low energy orientations being statistically favored. The Boltzmann averaged potential is a good approximation so long as the difference between the energies of any two orientations ω_1 and ω_2 is much less than kT,

$$|u_{\omega_1} - u_{\omega_2}| \ll kT. \quad (12)$$

We have performed test calculations of the induction and multipolar energy of several different polar adsorbates on graphite using angle explicit induction and multipole potentials instead of Eqs. (5)–(7). The parameters used in our computations can be found in "Comparison with atom-explicit potentials" section. For H_2O in the most favorable orientation the difference between the angle average and angle explicit potentials is about 10^{-3} kJ/mol, while for CO_2 the difference is about 0.1 kJ/mol. The largest difference between angle average and angle explicit potentials was noted for acetone, having an energy difference of about 0.3 kJ/mol at the potential minimum. However, the well depth for the acetone/graphite interaction potential is 35.57 kJ/mol, so that a difference of 0.3 kJ/mol is less than one percent of the total energy. The angle-averaged potentials are most accurate for nearly spherical molecules. Nevertheless, Eq. (12) is satisfied for all of the fluids listed in Table I at room temperature.

Self-consistency

We have not included polarization self-consistency in the derivation of the induction potentials, Eq. (8). This approximation simplified the derivations significantly. The dipole induced on carbon atom i in graphite due to dipoles on fluid molecules can be calculated from

$$\boldsymbol{\mu}_i^{\text{ind}} = \alpha_c(\mathbf{E}_i^f + \mathbf{E}_i^c), \quad (13)$$

where $\mathbf{E}_i^f$ is the electric field at i due to the fluid molecules and $\mathbf{E}_i^c$ is the local electric field resulting

TABLE I The Lennard–Jones (LJ) and multipole parameters for fluid–fluid potentials

	ε_{ff}/k (K)	σ_{ff} (Å)	μ_f (D)	Θ_f (10^{-40} C m^2)	Source
H_2O	78.02	3.152	1.85	–	[32]
NH_3	140	3.40	1.47	–	[33]
CO_2*	28.129(O)	2.757(O)	–	−12.2	[18]
	80.507(C)	3.033(C)			
Acetone†	85(methyl)	3.88(methyl)	2.70	–	[16]
	52.84(C)	3.75(C)			
	105.68(O)	2.96(O)			
N_2	96.42	3.663	–	−4.7	[34,35]
Cl_2	357	4.115	–	10.79	[34,36]
CO	110	3.59	0.112	−8.33	[34,35]
H_2S	250	3.73	0.97	–	[26,37]
SO_2	369.3	3.895	1.63	–	[34]
CS_2	488	4.438	–	12.0	[34,38]
C_2H_4	219	4.20	–	6.67	[34,35]
C_2H_5OH	327.8	4.575	1.69	–	[34]
N_2O	189	4.59	–	−11.67	[34,35]

*CO_2 is a three site LJ model. †Acetone is a four site LJ plus charge model.

from the induced dipoles on the other carbon atoms in graphite. We neglect induction effects on the fluid molecules in writing Eq. (13). For a single fluid molecule the total induction energy is

$$\boldsymbol{\mu}^{\text{ind}} = -\frac{1}{2}\sum_{i=1}^{N_c} \boldsymbol{\mu}_i^{\text{ind}} \cdot \mathbf{E}_i^{\text{f}}$$

$$= -\frac{1}{2}\sum_{i=1}^{N_c} \alpha_c(\mathbf{E}_i^{\text{f}} \cdot \mathbf{E}_i^{\text{f}} + \mathbf{E}_i^{\text{f}} \cdot \mathbf{E}_i^{\text{c}}), \qquad (14)$$

where summation is over all N_c carbon atoms in graphite. The first term inside the summation on the right hand side of Eq. (14) is the contribution from the permanent dipole on the fluid molecule and the second term comes from the field generated by the induced dipoles on the carbon atoms. $\mathbf{E}_i^{\text{c}}$ is given by [15]

$$\mathbf{E}_i^{\text{c}} = \sum_{k\neq i}^{N_c} \frac{1}{r_{ik}^3}\left[\frac{3\mathbf{r}_{ik}\cdot\boldsymbol{\mu}_k^{\text{ind}}}{r_{ik}^2}\mathbf{r}_{ik} - \boldsymbol{\mu}_k^{\text{ind}}\right], \qquad (15)$$

where $\mathbf{r}_{ik}$ is the vector from carbon atom k to carbon atom i, $\mathbf{r}_{ik} = \mathbf{r}_i - \mathbf{r}_k$. Note that $\mathbf{E}_i^{\text{c}}$ is dependent on $\boldsymbol{\mu}_i^{\text{ind}}$. The induced dipole on each carbon atom must be computed by iterating Eqs. (13) and (15) until $\boldsymbol{\mu}_i^{\text{ind}}$ converges.

We have performed test calculations for several different polar molecules on graphite and found self-consistency of the polarization term can be neglected. Taking acetone/graphite as an example, at 300 K the potential minimum with and without including polarization self-consistency are -35.85 and -35.57 kJ/mol, respectively. Note that the potential model we used for acetone has a dipole of 2.7 Debye, which makes it the most strongly polar molecule we studied in this paper. For less polar molecules the self-consistency effect at the potential energy minimum should be smaller in magnitude. This is consistent with previous work by Jedlovszky and Pàlinkàs [16] for bulk fluids. They compared polarizable and non-polarizable potentials for acetone. They found that the contribution from self-consistency is about 9% of the total energy for bulk liquid acetone at 298 K. The polarizability of acetone is 6.42 Å^3 whereas the polarizability of a carbon atom is only 1.76 Å^3 [17]. In this light, the polarization self-consistency in the induction term of the solid–fluid interaction is not expected to contribute significantly to the *total* energy (including both the bulk liquid and liquid–solid interaction) of the system given the smaller polarizability of the carbon atoms.

Comparison with Atom-explicit Potentials

We have calculated the interaction energies for H_2O/graphite, NH_3/graphite, and CO_2/graphite from the integrated expressions, Eqs. (8)–(10), and compared the results with the atomistic angle averaged potentials, Eqs. (5)–(7). The atom-explicit potentials used ten graphene layers, about 58 Å on a side, each containing 1080 carbon atoms. This system size was based on trial calculations and was found to contain more than enough atoms to accurately model the semi-infinite surface. For each calculation only a single adsorbate molecule was used (zero coverage limit). The fluid molecule was placed above the center of the graphite surface and the polar energy was computed by summing Eqs. (5)–(7) over all carbon atoms.

The LJ and electrostatic parameters for several polar molecules are given in Table I. There are often several different potential models available for a given molecule. Our goal in this work is to study the effect of including fluid–graphite polar interactions, so we have chosen the potential models in Table I rather arbitrarily; we have not attempted to identify the most accurate potential. The values of the parameters for carbon atoms in graphite are $\sigma_s = 0.340$ nm, $\varepsilon_s/k = 28.0$ K, $\Delta = 0.335$ nm, $\rho_s = 114\,\text{nm}^{-3}$ [18], $\Theta_c = -3.03\times10^{-40}$ C m^2 [6], and $\alpha_c = 1.76$ Å^3 [17]. We note that there are several theoretical values available for α_c, ranging from 1.58 to 1.76 Å^3 [17,19,20]. We have arbitrarily chosen the value of 1.76 Å^3 in our calculations. We found that using $\alpha_c = 1.58$ Å^3 did not substantially change the results of the simulations. Note that since Θ_c always appears as squared in Eqs. (5)–(10) we are not concerned about the sign of the graphite quadrupole. The standard Lorentz–Berthelot rules were used to obtain the values of σ_{sf} and σ_{sf}. The results from the atom-explicit potentials Eqs. (5)–(7), were compared with the integrated potentials Eqs. (8)–(10).

In Figs. 2–4 we compare PES computed from the non-polar 10-4-3 potential, the integrated polar potentials, and the atom explicit polar potentials at 300 K, for H_2O, NH_3, and CO_2. The integrated expressions are in excellent agreement with the atom-explicit summation results. Taking the atom-explicit potentials as the standard, the errors in the integrated potentials are less than 1% over the range where energy is negative. We note, however, that the integrated potentials are biased with respect to the atom explicit potentials, always giving a slightly less attractive potential.

The contributions to the solid–fluid potential energy at the potential minimum are tabulated in Table II for several fluid molecules at 300 K (note that Eqs. (9) and (10) depend on T). The contributions to the total potential energy (U_t) from the 10-4-3 (U_{LJ}), induction ($U_{\mu i}$), dipole–quadrupole ($U_{\mu\Theta}$), and quadrupole–quadrupole ($U_{\Theta\Theta}$) are evaluated at z_{min}, the minimum in U_t. For strongly polar molecules like H_2O and NH_3, the dipole-induced

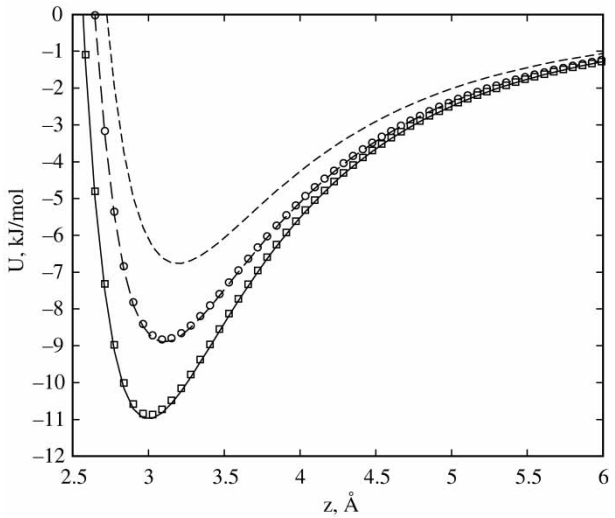

FIGURE 2 The H_2O/graphite potential at 300 K calculated using various approximations. The dotted line only includes the 10-4-3 potential Eq. (4), the dashed line is 10-4-3 plus atom explicit induction from Eq. (5), the circles are from 10-4-3 plus the integrated induction term Eq. (8), the solid line is the dashed line plus atomistic angle averaged quadrupole–dipole interactions from Eq. (6), and the squares are the circles plus the integrated quadrupole–dipole interactions, Eq. (9).

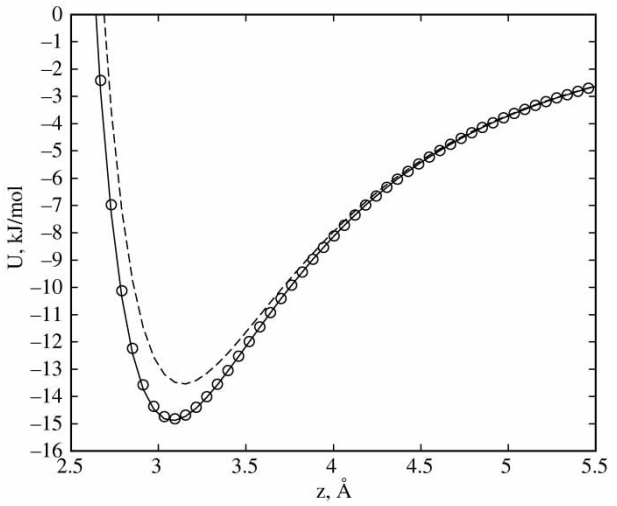

FIGURE 4 The CO_2/graphite potential at 300 K. The dotted line is computed from the 10-4-3 potential, Eq. (4), the solid line is the dotted line plus the atomistic angle averaged quadrupole–quadrupole interaction from Eq. (7), and the circles are the dotted line plus the integrated quadrupole–quadrupole interaction term from Eq. (10). The CO_2 molecular axis is oriented parallel to the graphite surface for the 10-4-3 calculations.

dipole and dipole–quadrupole interactions contribute significantly to the total energy. For CO_2, the quadrupole–quadrupole interaction is about 10% of the total energy at the PES minimum.

For the H_2O/graphite system the induction and dipole–quadrupole terms add about -4.7 kJ/mol to the total energy at the PES minimum (see Table II), which is about 40% of the total energy on the basis of the H_2O potential model we employed. The percentage will, of course, depend on the details of the fluid potential employed in the calculation. Gale and Beebe measured heats of adsorption of H_2O on carbon blacks, finding values between 18.8 and 25.1 kJ/mol [21]. It is likely that these values reflect functional groups and defects in the carbon black, rather than the inherent value for graphite. Theoretical values for the binding energy of H_2O on graphite have been computed by Avgul and Kiselev ~ -16 kJ/mol [8], Vernov and Steele ~ -7.47 kJ/mol [5], and by Feller and Jordan -24.3 kJ/mol [22] The potential used in this work gives a value of -10.98 kJ/mol. The polar contributions to the total energy help bring the potential into closer agreement with the *ab initio* calculated value of -24.3 kJ/mol [22], but the binding energy

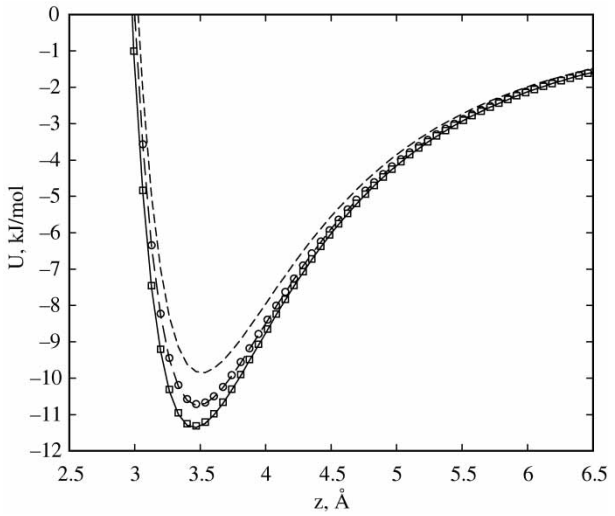

FIGURE 3 The NH_3/graphite potential at 300 K. The symbols and lines have the same meaning as in Fig. 2.

TABLE II Contributions due to non-polar and polar interactions to the fluid–graphite potential at the potential minimum for the fluid potentials from Table I

	U_t	U_{LJ}	$U_{\mu i}$	$U_{\mu\Theta}$	$U_{\Theta\Theta}$
H_2O	−10.98	−6.31	−2.49	−2.18	–
NH_3	−11.35	−9.82	−0.92	−0.61	–
CO_2*	−14.88	−13.48	–	–	−1.40
Acetone†	−35.57	−30.70	−3.03	−1.84	–
N_2	−9.00	−8.91	–	–	−0.09
Cl_2	−20.45	−19.75	–	–	−0.30
CO	−9.61	−9.29	−0.005	−0.004	−0.32
H_2S	−15.27	−14.64	−0.38	−0.25	–
SO_2	−20.35	−18.74	−0.92	−0.54	–
CS_2	−25.70	−25.46	–	–	−0.24
C_2H_4	−15.98	−15.88	–	–	−0.10
C_2H_5OH	−22.85	−21.73	−0.75	−0.38	–
N_2O	−16.78	−16.57	–	–	−0.21

* CO_2 molecular axis is parallel to the surface. † Acetone molecular plane is parallel to the surface. The temperature is 300 K and energies are in kJ/mol. U_{LJ} is computed from Eq. (4), $U_{\mu i}$ from Eq. (8), $U_{\mu\Theta}$ from Eq. (9), and $U_{\Theta\Theta}$ from Eq. (10).

from this model potential is still substantially weaker than the *ab initio* value.

The dominant contribution to the energy in Eqs. (8)–(10) comes, not surprisingly, from the first term in each equation, which accounts for the interactions with the surface graphene sheet in graphite. The summation over the deeper layers is accounted for by the second term in each of the equations, which contains the Δ term. This second term is typically only about 5% of the polar interaction energy near the PES minimum. Therefore, retaining only the first terms in Eqs. (8)–(10) is a very good approximation for most fluid–graphite systems.

Comparison With the Image Potential Approximation

Another method for computing the dipole-induced dipole interaction of an adsorbate molecule with a polarizable adsorbent is the image charge potential approximation [23,24]. The image charge potential is given by

$$U_{\mu i}(z) = -\frac{\mu_f(1+\cos^2\theta)}{16(4\pi\varepsilon_0)(z-\delta)^3}, \qquad (16)$$

where θ is the angle between the direction of the dipole moment of the adsorbate molecule and the surface normal and δ is the distance of the image charge from the surface. It is a common approximation to take the value of θ to be zero. The largest uncertainty in Eq. (16) is in the value of δ. The recommended value of δ for graphite is half the distance between graphene layers, $\delta = (1/2)\Delta$ [23,24]. If we equate (16) to Eq. (8), we can solve for the value of δ that gives the same value of $U_{\mu i}$ as Eq. (8). Considering the simple case where the z^{-4} term in Eq. (8) dominates, δ is then given by

$$\delta(z) = z - \left(\frac{z^4\varepsilon_0}{\alpha_c\rho_s\Delta}\right)^{\frac{1}{3}}. \qquad (17)$$

It can be seen from Eq. (17) that for graphite the value of δ is not a constant, but depends on the distance between the fluid dipole and the surface. We calculated $U_{\mu i}$ from Eqs. (8) and (16) for several different fluid molecules. As an example, the induction energies for H_2O/graphite computed from Eqs. (8) and (16) are plotted in Fig. 5. We have found that in most cases the image charge potential overestimates the induction energy near the potential minimum. The image charge potential is indistinguishable from the integrated induction potential for $z > 4.5$ Å. This emphasizes that the image potential is not appropriate for simulation of adsorption, since the adsorbate molecules in the monolayer are in close proximity to the surface.

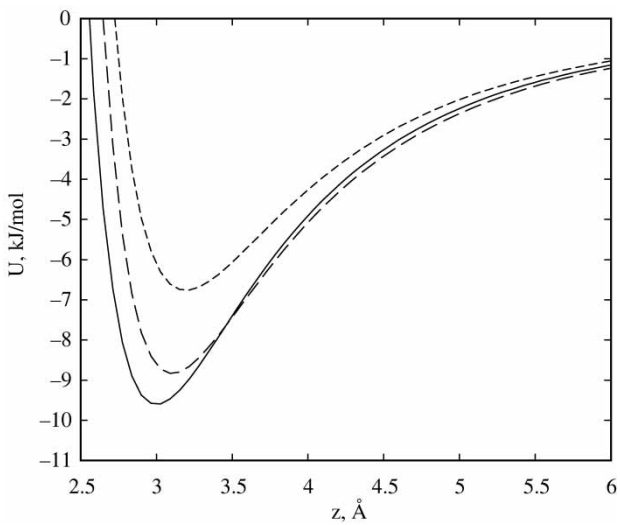

FIGURE 5 The contribution to the H_2O/graphite potential due to dipole-induced dipole interactions as calculated from the integrated induction expression of Eq. (8) (dashed line) and the image potential of Eq. (16) (solid line). The 10-4-3 potential is given by the dotted line. Note that the image potential method substantially overestimates the induction potential at short distances.

APPLICATIONS

Isosteric Heat of Adsorption at Zero Coverage

We have computed the zero coverage isosteric heat of adsorption for a number of different polar molecules on graphite in order to assess the importance of multipole and induction terms. The isosteric heat of adsorption at zero coverage, q_{st}^0, is computed from [25]

$$q_{st}^0 = RT - N_a \frac{\int_V u_s(\mathbf{r},\omega)\exp[-\beta u_s(\mathbf{r},\boldsymbol{\omega})]d\mathbf{r}\,d\boldsymbol{\omega}}{\int_V \exp[-\beta u_s(\mathbf{r},\boldsymbol{\omega})]d\mathbf{r}\,d\boldsymbol{\omega}}, \qquad (18)$$

where u_s is the interaction energy between the graphite surface and a molecule located at position $\mathbf{r}$ with orientation $\boldsymbol{\omega}$, $\beta = 1/kT$ and N_a is Avogadro's number. We used a Monte Carlo integration method with 1×10^7 trial insertions in order to evaluate the integral. Calculations were carried out using Eq. (4), both with and without polar terms, Eqs. (8)–(10).

The zero coverage isosteric heats of adsorption for several fluids are given in Table III. It can be seen from the table that in most cases, the interaction involving the quadrupole of fluids can be neglected. The only exception is CO_2, for which the quadrupole–quadrupole interaction accounts for about 10% of the total energy at the PES minimum. Note that there are molecules listed in Table III with quadrupole moments close to that of CO_2 (Cl_2, CS_2, and N_2O), yet for these molecules (Eq. 10) does not have much of an effect on the value of q_{st}^0. The reason for this is that the CO_2 model used is a non-spherical model, having three LJ sites, allowing the CO_2

TABLE III Isosteric heats at zero coverage on graphite in kJ/mol for the fluid potentials from Table I

	μ_f (D)	Θ_f (10^{-40}C m^2)	10-4-3	10-4-3 +polar terms
H_2O	1.85	–	3.32	5.58
NH_3	1.47	–	4.84	6.63
CO_2	–	−12.2	11.50	13.04
Acetone	2.70	–	31.9	36.80
N_2	–	−4.7	4.28	4.28
Cl_2	–	10.79	20.02	20.11
CO	0.112	−8.33	4.58	4.79
H_2S	0.97	–	12.30	13.34
SO_2	1.63	–	16.85	20.08
CS_2	–	12.0	26.46	26.71
C_2H_4	–	6.67	13.99	14.35
C_2H_5OH	1.69	–	22.62	23.35
N_2O	–	−11.67	15.02	15.20

μ_f and Θ_f are the fluid dipole and quadrupole moments, respectively, 10-4-3 values are computed from Eq. (4), and 10-4-3 + polar terms includes contributions from Eqs. (8)–(10), as appropriate.

molecule to approach the graphite surface more closely than an effective spherical model. This in turn means that the quadrupole–quadrupole term has a much larger effect on the PES, since Eq. (10) is roughly proportional to z^{-8}. The other molecules with large quadrupole moments reported in Table III all utilize effective spherical LJ potentials and hence the quadrupole–quadrupole terms are smaller for those models. In general, one should compute the contribution to the total energy due to the quadrupole–quadrupole interactions near the potential minimum in order to assess the importance of including this term in calculation of isosteric heats.

Equations (8) and (9) make substantial contributions to the total energy for molecules with large dipole moments. Note that these equations are longer ranged than the quadrupole–quadrupole term, so even SO_2, with a spherical effective LJ potential, has a sizable contribution from the polar terms. The spherical model for ethanol, however, is too unrealistic and as a result the polar terms are unimportant. This will not be the case for a multi-site model for ethanol. As a conservative rule of thumb, polar interactions should be included for any fluid with a dipole moment greater than about 1 Debye. Ignoring polar terms for fluids with dipole moments greater than 1 Debye will generally result in errors in q_{st}^0 of 10% or more.

Adsorption Isotherms

We have performed calculations to assess the influence of polar interactions on adsorption isotherms. Two fluids, acetone and H2S, were chosen as typical examples of strongly and weakly polar fluids, respectively. The dipole moment of acetone is 2.70 Debye, while that of H_2S is 0.97 Debye. The details of the potential models for these two fluids can be found in Refs. [16,26].

Molecular simulations were carried out in the Grand Canonical Monte Carlo (GCMC) ensemble [27]. Conventional GCMC works well for H_2S. However, insertion and deletion of molecules is extremely inefficient for simulation of acetone adsorption on graphite. We implemented the orientationally biased GCMC technique [28] to improve the efficiency of the acetone adsorption calculations. Each attempted insertion or deletion of a molecule utilized information from five random orientations. All the GCMC simulations were performed at 150 K. This temperature is probably too low to justify the use of the angle-averaged potential for acetone according to the criterion given in "Discussion on the angle average approach" section. However, we are focusing on the 1–2 layering transition. The angle-averaged potential will be quite accurate in the second layer at 150 K. A typical simulation run included 50 million moves for equilibration and an additional 50 million production moves. Displacements, reorientations, insertions, and deletions were attempted with equal probability. The average number of molecules in the simulation box varied from about 90 to 200. The potential cutoff was set to about 10 Å.

Adsorption isotherms for acetone on graphite at 150 K are presented in Fig. 6. The circles are simulation results computed from the non-polar 10-4-3 potential only and the squares include polar interactions through the integrated expressions (8)–(10). It can be seen that the addition of polar interactions changed the character of the 1–2 layering transition from continuous to apparently first-order. However, the pressure at which the transition occurs is not significantly altered by inclusion of the polar terms. This observation is

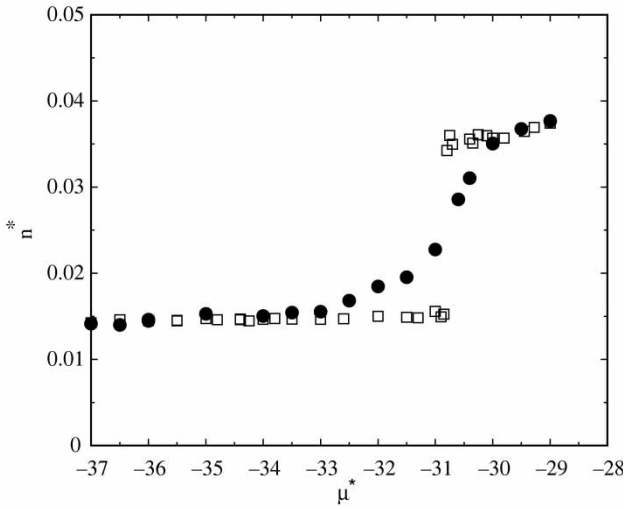

FIGURE 6 Adsorption isotherms for acetone on graphite at 150 K. The squares are the simulations using Eq. (4) plus Eqs. (8) and (9). The circles are the simulations using Eq. (4) only. The chemical potential μ^* and coverage n^* are in arbitrary units.

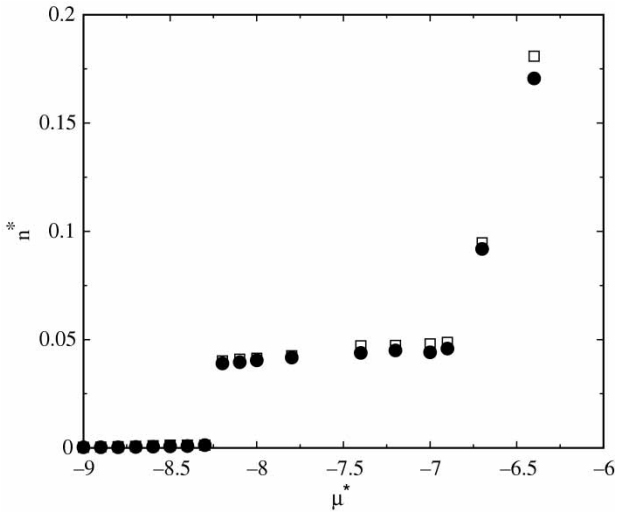

FIGURE 7 Adsorption isotherm of H_2S on graphite at 150 K. The symbols have the same meaning as in Fig. 6.

consistent with previous observations showing that an increase or decrease in the solid–fluid potential can change the character of the 1–2 layering transition without greatly affecting the pressure at which the transition takes place [29].

The isotherms of H_2S on graphite at 150 K computed from the non-polar potential and the full potential including polar interactions are plotted in Fig. 7. It can be seen that shape of the isotherm and apparent order of the 1–2 layering transition are insensitive to the inclusion of polar interactions in this case. Thus, polar interactions of H_2S with graphite may be safely ignored. In general, isotherms for weakly polar fluids may be computed accurately without including polar terms in the solid–fluid interaction potential, while for strongly polar fluids require inclusion of these terms for high accuracy. We were unable to observe any layering transitions in H_2O/graphite isotherms over the temperature range of 200–300 K. This is consistent with the recent estimation by Gatica *et al.*, that the wetting temperature for water on graphite is probably close to 500 K [30].

CONCLUSION

We have derived approximate angle averaged integrated expressions for including dipole-induced dipole, dipole–quadrupole, and quadrupole–quadrupole interactions in molecular simulations of polar and quadrupolar molecules interacting with graphite. These expressions provide a first-order method of including corrections due to the polarizability and presence of quadrupoles in graphite. These effects are currently almost always ignored when computing adsorption of polar molecules on graphite. The integrated potential functions depend only on the distance between a fluid molecule and the graphite surface. They are simple, easy to implement into computer simulations, and computationally inexpensive. The potential energy calculated from Eqs. (8)–(10) agrees well with the results from calculations from atomistic potentials. We have neglected self-consistency in the polarization expression (8), but we believe that this effect is relatively small.

Calculations on several polar fluids were used to test the derived formulas. It was found that for weakly polar fluids, like H_2S, the solid–fluid polar terms are negligible compared with the LJ interactions. For strongly polar fluids, such as H_2O and acetone, the contribution from the polar terms to the total potential energy is significant and must be included for accurate calculations.

The derived formulas were used in calculation of the zero coverage isosteric heat of adsorption for several different polar fluids on graphite and compared with the values computed from the non-polar potential. For strongly polar fluids the electrostatic and induction interactions increase the heat of adsorption substantially. GCMC simulations were performed to test the influence of polar interactions on adsorption isotherms. Addition of polar interactions to solid–fluid potential can change the character of the 1–2 layering transition for strongly polar fluids adsorbing on graphite. In closing, we note that we have ignored three-body interactions which have been shown to be on the order of 20% for rare gas atoms adsorbed on the surface of graphite [31]. Very accurate calculations must take these terms into account.

Acknowledgements

This work was supported by NSF under Grant No. EEC 0085480. Calculations were performed at the Center for Molecular and Materials Simulations at the University of Pittsburgh. We thank L. W. Bruch, M. W. Cole, R. F. Cracknell, and K. D. Jordan for helpful comments.

References

[1] Steele, W.A. (1973) "The physical interaction of gases with crystalline solids. I. Gas–solid energies and properties of isolated adsorbed atoms", *Surf. Sci.* **36**, 317–352.
[2] Steele, W.A. (1993) "Molecular interactions for physical adsorption", *Chem. Rev.* **93**, 2356–2378.
[3] Nicholson, D., Cracknell, R.F. and Parsonage, N.G. (1990) "Evaluation of a model potential function for Ar graphite interaction using computer simulation", *Mol. Simul.* **5**, 307–314.
[4] Cracknell, R.F. (1990) Ph.D. thesis, Imperial College (London).
[5] Vernov, A. and Steele, W.A. (1992) "The electrostatic field at a graphite surface and its effect on molecule–solid interactions", *Langmuir* **8**, 155–159.
[6] Whitehouse, D.B. and Buckingham, A.D. (1993) "Experimental determination of the atomic quadrupole moment of graphite", *J. Chem. Soc., Faraday Trans.* **89**, 1909–1913.

[7] Hansen, F.Y., Bruch, L.W. and Roosevelt, S.E. (1992) "Electrostatic forces and the frequency spectrum of a monolayer solid of linear molecules on graphite", *Phys. Rev. B* **45**, 11238–11248.
[8] Avgul, N.N. and Kiselev, A.V. (1970) "Physical adsorption of gases and vapors of graphitized carbon blacks", In: Walker, Jr., P.L., eds, *Chemistry and Physics of Carbon* (Marcel Dekker, New York), Vol. 6, pp 1–124.
[9] Chen, R., Trucano, P. and Stewart, R.F. (1977) "The valence-charge density of graphite", *Acta Crystallogr. A Crystal Phys. Diffraction, Theoret. General Crystallogr.* **33**, 823–828.
[10] Steele, W.A. (1974) *The Interaction of Fluids with Solid Surfaces* (Pergamon, Oxford).
[11] Jiang, S.Y., Gubbins, K.E. and Zollweg, J.A. (1993) "Adsorption, isosteric heat and commensurate–incommensurate transition", *Mol. Phys.* **80**, 103–116.
[12] Cracknell, R.F., Nicholson, D. and Quirke, N. (1993) "A Grand Canonical Monte Carlo study of Lennard–Jones mixtures in slit shaped pores", *Mol. Phys.* **80**, 885–897.
[13] Nicholson, D. and Gubbins, K.E. (1996) "Separation of carbon dioxide-methane mixtures by adsorption: effects of geometry and energetics on selectivity", *J. Chem. Phys.* **104**, 8126–8134.
[14] Hirschfelder, J.O., Curtiss, C.F. and Bird, R.B. (1954) *Molecular Theory of Gases and Liquids* (John Wiley & Sons, New York).
[15] Chialvo, A.A. and Cummings, P.T. (1996) "Engineering a simple polarizable model for the molecular simulation of water applicable over wide ranges of state conditions", *J. Chem. Phys.* **105**, 8274–8281.
[16] Jedlovszky, P. and Pálinkás, G. (1995) "Monte Carlo simulation of liquid acetone with a polarizable molecular model", *Mol. Phys.* **84**, 217–233.
[17] Miller, T.M. and Bederson, B. (1977) In: Bates, D.R. and Bederson, B., eds, *Advances in Atomic and Molecular Physics* (Academic Press, London), Vol. 13, pp 1–55.
[18] Harris, J.G. and Yung, K.H. (1995) "Carbon dioxide's liquid–vapor coexistence curve and critical properties as predicted by a simple molecular model", *J. Phys. Chem.* **99**, 12021–12024.
[19] Carlos, W.E. and Cole, M.W. (1980) "Interaction between a He atom and a graphite surface", *Surf. Sci.* **91**, 339–357.
[20] Crowell, A.D. and Brown, J.S. (1982) "Laterally averaged interaction potentials for $^1H_2$ and $^2H_2$ on the (0001) graphite surface", *Surf. Sci.* **123**, 296–304.
[21] Gale, R.L. and Beebe, R.A. (1964) "Determination of heats of adsorption on carbon blacks and bone mineral by chromatography using the eluted pulse technique", *J. Phys. Chem.* **68**, 555–567.
[22] Feller, D. and Jordan, K.D. (2000) "Estimating the strength of the water/single-layer graphite interaction", *J. Phys. Chem. A* **104**, 9971–9975.
[23] Wang, Z.M. and Kaneko, K. (1995) "Dipole oriented states of SO_2 confined in a slit-shaped graphitic subnanospace from calorimetry", *J. Phys. Chem.* **99**, 16714–16721.
[24] Crowell, A.D. (1968) "van der Waals potentials for simple polar molecules interacting with graphite", *J. Chem. Phys.* **49**, 892–895.
[25] Nicholson, D. and Parsonage, N.G. (1982) *Computer Simulation and the Statistical Mechanics of Adsorption* (Academic Press, London).
[26] Kristof, T. and Liszi, J. (1997) "Effective intermolecular potential for fluid hydrogen sulfide", *J. Phys. Chem. B* **101**, 5480–5488.
[27] Allen, M.P. and Tildesley, D.J. (1987) *Computer Simulation of Liquids* (Clarendon Press, Oxford).
[28] Smit, B. (1995) "Grand canonical Monte Carlo simulations of chain molecules: adsorption isotherms of alkanes in zeolites", *Mol. Phys.* **85**, 153–172.
[29] Zhao, X.C., Kwon, S.J., Vidic, R., Borguet, E. and Johnson, J.K. (2002) "Layering and orientational ordering of propane on graphite: An experimental and simulation study", *J. Chem. Phys.* **117**, 7719–7731.
[30] Gatica, S.M., Johnson, J.K., Zhao, X.C. and Cole, M.W. (2004) "Wetting transition of water on graphite and other surfaces", *J. Phys. Chem. B*, **108**, 11704–11708.
[31] Kim, H.-Y. and Cole, M.W. (1987) "Three-body contribution to the adsorption potential of atoms on graphite", *Phys. Rev. B* **35**, 3990–3994.
[32] Jorgensen, W.L., Chandrasekhar, J., Madura, J.D., Impey, R.W. and Klein, M.L. (1983) "Comparison of simple potential functions for simulating liquid water", *J. Chem. Phys.* **79**, 926–935.
[33] Ferrario, M., Haughney, M., McDonald, I.R. and Klein, M.L. (1990) "Molecular-dynamics simulation of aqueous mixtures: Methanol, acetone, and ammonia", *J. Chem. Phys.* **93**, 5156–5266.
[34] Rowley, R.L. (1994) *Statistical Mechanics for Thermophysical Property Calculations* (Prentice Hall, Englewood Cliffs, NJ).
[35] Buckingham, A.D., Disch, R.L. and Dunmur, D.A. (1968) "Quadrupole moments of some simple molecules", *J. Am. Chem. Soc.* **90**, 3104–3107.
[36] Buckingham, A.D., Graham, C. and Williams, J.H. (1983) "Electric field-gradient-induced birefringence in dinitrogen, ethane, cyclopropane, dichlorine, nitrous oxide, and methyl fluoride", *Mol. Phys.* **49**, 703–710.
[37] *CRC Handbook of Chemistry and Physics*, 80 ed. (CRC Press, Boca Raton, 1999).
[38] Battaglia, M.R., Buckingham, A.D., Neumark, D., Pierens, R.K. and Williams, J.H. (1981) "The quadrupole moments of carbon dioxide and carbon disulfide", *Mol. Phys.* **43**, 1015–1020.